Mutation of a Putative Sperm Membrane Protein in *Caenorhabditis elegans* Prevents Sperm Differentiation but Not Its Associated Meiotic Divisions

Steven W. L'Hernault and P. Michele Arduengo

Department of Biology, Emory University, Atlanta, Georgia 30322

Abstract. Spermatogenesis in the nematode *Caenorhabditis elegans* uses unusual organelles, called the fibrous body-membranous organelle (FB-MO) complexes, to prepackage and deliver macromolecules to spermatids during cytokinesis that accompanies the second meiotic division. Mutations in the *spe-4* (*sper*matogenesis-defective) gene disrupt these organelles and prevent cytokinesis during spermatogenesis, but do not prevent completion of the meiotic nuclear divisions that normally accompany spermatid formation. We report an ultrastructural analysis of *spe-4* mutant sperm where the normally close association of the FB's with the MO's and the double layered membrane surrounding the FB's are both defective. The internal membrane structure of the MO's is also disrupted in *spe-4* mutant sperm. Although sperm morphogenesis in *spe-4* mutants arrests prior to the formation of spermatids, meiosis can apparently be completed so that haploid nuclei reside in an arrested spermatocyte. We have cloned the *spe-4* gene in order to understand its role during spermatogenesis and the molecular basis of how mutation of this gene disrupts this process. The *spe-4* gene encodes an ~1.5-kb mRNA that is expressed during spermatogenesis, and the sequence of this gene suggests that it encodes an integral membrane protein. These data suggest that mutation of an integral membrane protein within FB-MO complexes disrupts morphogenesis and prevents formation of spermatids but does not affect completion of the meiotic nuclear divisions in *C. elegans* sperm.

DEVELOPMENT of sperm in the nematode *Caenorhabditis elegans* offers a number of advantages as a model system for studies of cellular morphogenesis. Spermatogenesis occurs via a series of steps that are cytologically distinct, and these stages occur sequentially along the length of the gonad. Additionally, many aspects of spermatogenesis will occur in vitro and many genes in which mutations specifically arrest spermatogenesis have been recovered. The mature spermatozoon that results from this differentiation pathway has a single pseudopod and moves by crawling on the substrate; nematode sperm lack both a flagellum and acrosome (for review see Kimble and Ward, 1988).

Unequal partitioning of cellular constituents during cell division can play an important role during development (for review see Davidson, 1986). In *C. elegans*, unequal cytoplasmic partitioning occurs at several stages during spermatogenesis. During meiosis II, for instance, part of the system that ensures the orderly segregation of components to the spermatid are unusual organelles called the fibrous-body membranous organelle (FB-MO)[1] complexes. Several of the genes in which mutations disrupt aspects of spermatogenesis (*sper*matogenesis-defective) do so by affecting cytoplasmic partitioning (Hirsh and Vanderslice, 1976; Ward, 1986; Ward and Miwa, 1978; Argon and Ward, 1980; Edgar, 1982; Burke, 1983; Sigurdson et al., 1984; L'Hernault et al., 1988; Shakes, 1988, 1989*a*,*b*). Several *spe* mutants have defects in formation and/or function of the FB-MO complexes and a subset of these mutants also prevent formation of haploid spermatids (Ward et al., 1981; Shakes and Ward, 1989*b*; Varkey, J., and S. Ward, unpublished observations).

Mutations in the *spe*-4 gene disrupt the coordination of cytokinesis with meiotic nuclear divisions during spermatogenesis so that a spermatocyte-like cell that contains four haploid nuclei forms instead of four spermatids (L'Hernault et al., 1988). In this paper, we present electron microscopic analysis showing that developing *spe-4* spermatocytes contain abnormal FB-MO complexes. An allele specific restriction fragment length polymorphism (RFLP) and transgenic rescue have been used to localize and clone the *spe-4* gene. Molecular analysis suggests that *spe-4* encodes a 465 amino acid integral membrane protein that is expressed during spermatogenesis. We suggest that, as a likely FB-MO complex protein, the *spe-4* product might play a role in spermatid formation during meiosis II.

1. *Abbreviations used in this paper*: FB-MO, fibrous body-membranous organelle; MSP, major sperm protein; PCR, polymerase chain reaction; RFLP, restriction fragment length polymorphism.

Materials and Methods

Strains

Culture, manipulation of worms, and genetic analyses were performed by standard methods (Brenner, 1974). All strains used in this work (except *spe-4[q347]*) (see below) were derived from the wild type *C. elegans* strain var. Bristol N2. Strains were from the Cambridge collection (Brenner, 1974), except as noted below. Recovery and preliminary analysis of two ethyl methane sulfonate induced alleles of *spe-4, hc78,* and *hc81,* have been described previously (L'Hernault et al., 1988). The *spe-4* allele *q347* was isolated on a Bristol chromosome and provided by T. Schedl (Washington University School of Medicine, St. Louis, MO). This *spe-4* mutation arose spontaneously during outcrossing of *gld-1(q343)* to N2; *gld-1(q343)* was induced in a TR679 *mut-2 (r457)* background (Collins et al., 1987). Standard *C. elegans* nomenclature has been used throughout this paper (Horvitz et al., 1979). Genetic markers used are LGI, *unc-13(e51, e1091), unc-15(e73), dpy-5(e61),* and *sDf6* (Rose and Baillie, 1980); LGIV, *fem-1(hc17*ts) (Nelson et al., 1978), *fem-3(q23*gf) (Barton et al., 1987); LGV, *him-5(e1490)* (Hodgkin et al., 1979). The mutation *sDf5* (Rose and Baillie, 1980), the translocation *nDp4* (Thomas, J., and H. R. Horvitz, unpublished observations), or the mutation *gld-1(q268)* (Schedl, T., and J. Kimble, unpublished observations) were used to balance and maintain the heterozygous *spe-4* strains used in this study.

Worm Culture

Routine handling of worms was performed at 20°C in petri plates filled with agar and seeded with *Escherichia coli* OP50 (Brenner, 1974). Worms to be used for DNA preparation were raised on 9-cm agarose plates seeded with *E. coli* P90C (Miller et al., 1977; Fire, 1986). Worms to be used for RNA preparation were raised in liquid culture and synchronized by hypochlorite treatment (Nelson et al., 1982). Animals with a female soma and containing oocytes, but no sperm, were recovered from cultures of *fem-1(hc17)* that were raised at 25°C (Nelson et al., 1978). Animals with a female soma and containing sperm, but no oocytes, were recovered from cultures of *fem-3(q23)* that were raised at 25°C (Barton et al., 1987). Males from *him-5* liquid cultures were prepared as described previously (Klass and Hirsh, 1981; Nelson et al., 1982).

Phenotypic Analyses

Testes were released by hand-dissecting males in SM buffer, pH 7.8, and analyzed as described previously (Nelson and Ward, 1980); SM contains 50 mM NaCl, 25 mM KCl, 5 mM $CaCl_2$, 1 mM $MgSO_4$, and 5 mM Hepes. Dpy males obtained from *sDf5/spe-4 dpy-5* balanced lines were used for these phenotypic analyses. Testes and sperm from all three *spe-4* mutants were examined; they were highly similar (see below). Control experiments were performed on F_1 Dpy males produced by mating *dpy-5/+* males to *dpy-5* hermaphrodites; these and previous analyses (L'Hernault et al., 1988) indicate that *dpy-5* sperm are indistinguishable from N2 wild type. In this paper, the final cellular stage accumulated during *spe-4* spermatogenesis is called the terminal spermatocyte.

Testes and sperm were prepared for transmission EM essentially as described previously (Shakes and Ward, 1989*a*) except that samples were embedded for thin sectioning in LX112 (Ladd Research Industries Inc., Burlington, VA).

Nucleic Acid Methods

DNA was prepared from mixed populations of worms by a modification of previous procedures designed for worms grown on plates (Wood, 1988). RNA was isolated as previously described (Burke and Ward, 1983; Rosenquist and Kimble, 1988). General methods for manipulation of DNA and RNA were from Sambrook et al. (1989) and Ausubel et al. (1989). Plasmid DNA for worm microinjections was prepared and purified by chromatography on Qiagen resin according to the manufacturer's instructions (Qiagen Inc., Chatsworth, CA).

Southern and Northern blots were prepared using Hybond N (Amersham Corp., Arlington Heights, IL), and DNA probes were labeled by random hexamer priming as described by Sambrook et al. (1989). Hybridizations and subsequent washing protocols followed Church and Gilbert (1984) and were performed at 65°C.

Primer extension and RNA polymerase chain reaction (PCR) experiments were performed to determine the 5' end of the *spe-4* transcript. The RNA used for either of these techniques was from male *him-5* worms, *fem-3* worms raised at 25°C (which have a female soma but a male germline), and, as a negative control, *fem-1* worms raised at 25°C (which have a female soma and germline). Primer extension was performed by using a 5' end ^{32}P-labeled antisense oligonucleotide of 30 bases (primer #2, Table I) that was annealed to either 1 μg of polyA+ or 20 μg of total RNA. Conditions used for primer extension were essentially as described in Sambrook et al. (1989). Sizes of primer extension DNA products were determined by comparison to DNA sequencing reactions in adjacent lanes on a 6% polyacrylamide/urea sequencing gel. RNA PCR was performed using the GeneAmp Thermostable rTth Reverse Transcriptase RNA PCR kit according to the manufacturer's instructions (Perkin Elmer Cetus, Norwalk, CT). Reverse transcriptase reactions included 250 ng total RNA primed with an antisense primer (Primer #3, Table I) and were incubated at 60°C for 10 min. PCR reagents and the sense primer (Primer #1, Table I) were then added to the first strand reverse transcription products and 35 cycles of PCR were performed, each with a 1-min 95°C denaturation step followed by a 1-min 53°C annealing/extension step. Resulting PCR products were fractionated by agarose gel electrophoresis.

Standard techniques were used for both DNA cloning and sequence analysis (Sambrook et al., 1989). Cosmids containing genomic DNA from the *unc-15* to *lin-10* interval of chromosome I were identified and recovered as part of the physical mapping of the *C. elegans* genome (Coulson et al., 1986, 1988) and generously provided by A. Coulson and J. Sulston (Medical Research Council, Laboratory of Molecular Biology, Cambridge, England). Restriction fragments from cosmids were fractionated on agarose gels, excised, and subcloned into Bluescript (Stratagene, La Jolla, CA) or M13mp18 (Yanisch-Perron et al., 1985). Two existing cDNA libraries prepared from polyA+ RNA from L4 stage enriched or mixed stage hermaphrodites (courtesy of J. Ahringer and J. Kimble, Laboratory of Molecular Biology, University of Wisconsin, Madison, WI; and R. Barstead and R. Waterston, Department of Genetics, Washington University School of Medicine, St. Louis, MO) were screened with genomic subclones. We recovered three cDNAs and the largest (from the R. Barstead and R. Waterston library) was completely sequenced.

PCR was performed with Taq polymerase (Perkin-Elmer/Cetus or

Table I. Single Stranded DNA Primers Used for Primer Extension and PCR

Primer	5' to 3' Sequence	Position in *spe-4* Sequence*
1	ATTACCTGTCTAAAAATGGACAC	1-23; Sense primer
2	CCAAATAGACAATGTCAGTGACATATTGGC	91-120; Antisense primer
3	CCAACTCCATTGATAAATCCATCC	213-222 and 223-236; Antisense primer
4	TTTGCCGTTTTAGCACCGATGGG	619-641; Sense primer
5	TCAGATGTTGACACAGTGGTGCT	1036-1058; Antisense primer
6	CGATACTATGTATTCTTTGCC	last 21 nt.'s; Antisense primer
7	GAAACAGCTATGACCATGATTAC	n.a.; Bluescript vector primer

* See Fig. 7 for the numbered positions of primers #1-5. Primer #3 hybridizes to the 5' end of exon 2 and the 3' end of exon 1; it has no homology to intron 1. Primer #6 is complementary to the last 21 nucleotides of genomic sequence printed in Fig. 7. Primer #7 includes the start codon of the β-galactosidase gene in Bluescript and can be used together with an appropriate second primer to PCR amplify inserts cloned into the polylinker of this vector.
n.a., not applicable.

Promega) on DNA samples either to localize the deletion in the *spe-4(q347)* allele or to verify the presence of cloned DNA in transgenic worms. Samples containing either 100 ng of genomic or 1 ng of cosmid DNA were amplified by PCR with primers #4 and 5 (see Table I) in order to characterize the *spe-4(q347)* deletion. 100 μl reactions were set up under standard conditions (Innis and Gelfand, 1990). 25 cycles were performed in a Perkin-Elmer DNA Thermal Cycler under the following conditions: denaturation at 94°C for one min, annealing at 63°C for two min, and extension at 72°C for one min. PCR products were fractionated by agarose gel electrophoresis and gel bands containing the desired PCR product were excised and pooled, and the contained DNA was purified with GeneClean (Biol01, La Jolla, CA) for direct sequencing.

PCR was also performed on small numbers of worms to characterize transgenic worms and various fertile and sterile *spe-4* homozygous controls. Worms were first picked to individual plates to verify if they were fertile or laid unfertilized oocytes. Worms of the appropriate genotype were then pooled and processed for PCR by the techniques of Barstead and Waterston (1991). Aliquots containing the DNA from eight worms were subjected to 30 cycles of PCR with primer #6 and either primer #1 or #7 (see Table I for primer positions) under the following conditions: denaturation at 94°C for one min, annealing at 53°C for two min, and extension at 72°C for one min. The resulting PCR products were fractionated by agarose gel electrophoresis.

DNA was sequenced by the chain termination method (Sanger et al., 1977) using T7 DNA polymerase (Sequenase II, U.S. Biochemicals, Cleveland, OH), and both double stranded templates in Bluescript and single stranded M13 templates were used. Sequencing was initiated from oligonucleotides complementary to previously determined sequences. One cDNA and the entire genomic region from which it was derived plus flanking regions at both ends were sequenced, the former on the sense strand and the latter on both strands. Sequences were compiled and analyzed using GENEPRO (Riverside Scientific, Bainbridge Island, WA) and FASTA (Pearson and Lipman, 1988).

Germline Transformation of C. elegans

Transformation of *C. elegans* by microinjection of recombinant plasmid DNA was carried out essentially as described by Mello et al. (1991). This technique involves a single, high-volume injection into the central cytoplasmic syncytium of each of the two distal gonadal arms. Worms were microinjected with either 100 μg/ml pOA1, which is a Bluescript recombinant plasmid that contains the *spe-4* gene (see Results) or 10 μg/ml pOA1 mixed with 100 μg/ml pRF4. The pRF4 plasmid contains *rol-6(su1006)II*, which confers a dominant rolling phenotype that aids in identifying worms that have been genetically transformed by the microinjection procedure (Mello et al., 1991). DNA for microinjection was suspended in 10 mM Tris-HCl, 1 mM EDTA (TE), pH 7.5.

The recessive nonconditional sterility exhibited by all *spe-4* mutants required that we microinject heterozygous non-Spe hermaphrodites, and then test for the effect of the transforming DNA on their Spe progeny. The recipient strain for all microinjections was *gld-1(q268)/unc-13(e1091)spe-4(q347)lin-10(e1439)*. Mutation of the *lin-10* gene prevents formation of a functional vulva so that embryos hatch within a *lin-10* mutant hermaphrodite, which is then devoured by its feeding progeny (Ferguson and Horvitz, 1985). This "bag of worms" phenotype associated with *lin-10* requires functional sperm, so *spe-4 lin-10* mutant hermaphrodites bloat with oocytes, but never form embryos and do not "bag". It was reasoned that transformation of *spe-4* should result in the "bag of worms" phenotype appearing in the paralyzed (due to *unc-13) unc-13 spe-4 lin-10* progeny of microinjected heterozygous parents. About 5% of *lin-10* hermaphrodites do not become "bags of worms" because they form a functional vulva, and these animals permit outcrossing to test a *spe-4* transgene in other genetic backgrounds. Outcrossing was performed with *sDf5/spe-4(q347)* heterozygous males in order to establish transgenic strains in which the *unc-13 lin-10* chromosomes were replaced by *spe-4* chromosomes. Pedigree analysis and PCR were performed in order to ensure that these strains contained the transgene.

Results

Review of C. elegans Spermatogenesis

Development of sperm in *C. elegans* males has been described in detail (Wolf et al., 1978; Ward et al., 1981; Ward, 1986; Kimble and Ward, 1988) and these cellular events are reviewed in Fig. 1. The primary spermatocyte initially forms in syncytium with a cytoplasmic core called the rachis. Before the meiotic divisions, the primary spermatocyte buds off the rachis and completes development without any requirement for intimate association with other cells. As in most cells, nuclear divisions are closely coordinated with cytokinesis and other aspects of cytodifferentiation. The primary spermatocyte undergoes the two nuclear divisions of meiosis to give rise to four haploid spermatids. These spermatids form by budding off of a residual body, and spermatids only contain a subset of cellular constituents present in the secondary spermatocyte. Material within the residual body, which includes all the ribosomes and most of the actin and tubulin, is apparently resorbed (Wolf et al., 1978; Ward et al., 1981; Nelson et al., 1982; Ward, 1986). Sessile spermatids, since they lack ribosomes, complete differentiation into motile spermatozoa in the absence of cellular protein synthesis (Ward et al., 1983).

The asymmetric partitioning of cellular constituents to the spermatids as they bud off of the residual body partly occurs via specialized organelles called the FB-MO complexes, and the morphogenesis of these structures is reviewed in Fig. 2 (Wolf et al., 1978; Ward et al., 1981; Ward, 1986; Roberts et al., 1986). The MO's begin to form from the Golgi apparatus in pachytene spermatocytes, and the FB's form a short time later in close association with the MO's (Fig. 2 *a*). Growth of the fibrous body in the primary spermatocyte occurs within the confines of a MO-derived membrane enve-

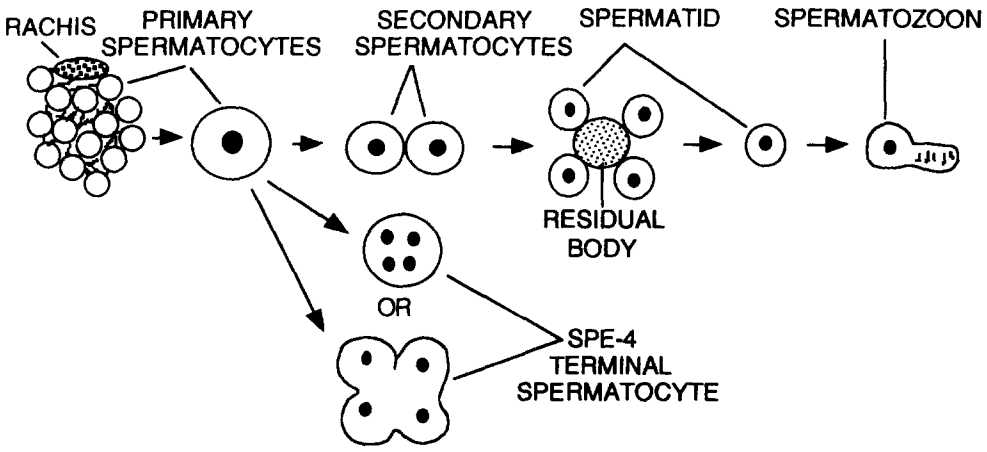

Figure 1. Summary of *C. elegans* spermatogenesis and how it is affected in *spe-4* mutants. For explanation see the text.

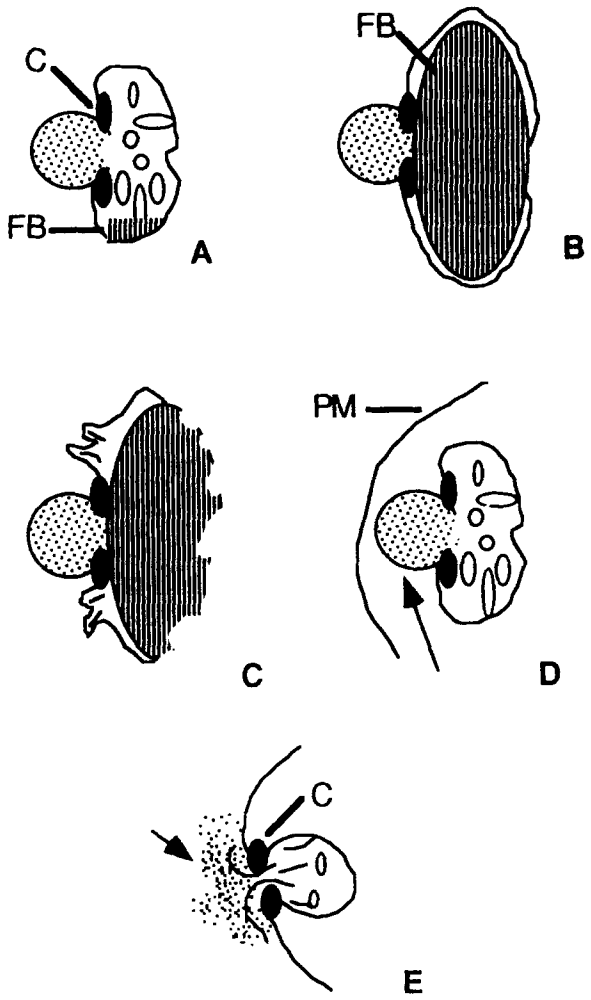

Figure 2. Summary of morphogenesis of the FB-MO complex. (*a*) The fibrous body (*FB*) develops in close association with, and is surrounded by the membranous organelle (*MO*) within the primary spermatocyte. The MO is separated by a collar (*C*) region into a head (specked region at left) and body (region to the right of the collar); (*b*) the FB-MO complex reaches its largest size within mature spermatocytes. The double layered MO-derived membrane surrounds the striped fibers within the FB, and the fibers of the FB contain MSP; (*c*) the membranes surrounding the FB retract and fold up as the FB begins to disappear and disperse its contents during budding of spermatids from the residual body; (*d*) the head of each MO (*arrow*) moves to a position just below the plasma membrane (*PM*) of the spermatid, and the FB's disappear; (*e*) the head of the MO fuses at the collar to the plasma membrane and exocytoses its contents (speckles at the arrow) onto the cell surface. A permanent fusion pore remains at the point of each MO fusion (each cell has many MO's).

lope (Fig. 2 *b*). These membrane-bounded structures contain many of the membrane and soluble components required by the spermatid; once the spermatid has completed separation from the residual body, the MO disassociates from the FB, the double membrane that surrounds the FB is retracted, and the fibrous contents, principally the major sperm protein (MSP), are dispersed throughout the cytoplasm (Fig. 2 *c*). The MO then becomes located just below the plasma membrane in the spermatid (Fig. 2 *d*). During spermiogenesis, when the spermatid is converted into the spermatozoon, membrane of each MO head fuses with the plasma membrane and deposits its contents on the cell surface; this occurs on the cell body surface and not on the pseudopodial surface (Fig. 2 *e*). In contrast, MSP from the FB localizes in the pseudopod (Ward and Klass, 1982) where it appears to play a role in the structure and motility of this cellular region (Roberts, 1983; Roberts et al., 1989; Sepsenwol et al., 1989).

Phenotypic Analyses of spe-4

In *spe-4* mutants, meiotic divisions, cytokinesis, and cytodifferentiation during spermatogenesis are not coordinated, resulting in a spermatocyte-like cell that contains four haploid nuclei (Fig. 1; also see L'Hernault et al., 1988). To understand the basis of this phenotype, we performed an ultrastructural analysis to examine the terminal phenotype of these *spe-4* spermatocytes and to determine how they differed from wild type. In wild type primary spermatocytes, the FB's develop in close association with the MO's and are enveloped by a double layered membrane as they form (Fig. 3 *a*). In *spe-4* primary spermatocytes, the membrane surrounding the FB's, when it is present, does not appear to be a double layered structure (Fig. 3 *b*). MO's in *spe-4* spermatocytes appear swollen and they either are not associated with FB's or, when they are, this association is not as prominent as in wild type (Fig. 3 *a*). Development of *spe-4* spermatocytes continues until a cell that is apparently arrested without completing spermatid formation is observed (Fig. 3, *d* and *h*). Occasionally, these cells will attempt to divide (Fig. 3 *h*) but, frequently, no evidence of cellular division is observed (Fig. 3 *d*). In *spe-4* mutant testes, many cells with these ultrastructural abnormalities accumulate, suggesting that this is the terminal phenotype. The MO's can be grossly swollen in the terminal spermatocyte and still lack any obvious association with FB's (Fig. 3, *d*, *g*, and *h*). The FB's present in *spe-4* terminal spermatocytes are frequently not surrounded by membrane (Fig. 3, *d* and *h*) but, occasionally, small patches of membrane that never completely surround the FB are observed (data not shown). In contrast, during wild type spermatogenesis, FB-MO complexes segregate to spermatids

Figure 3. Aberrant morphogenesis of the FB-MO complexes in *spe-4* mutants. (*A* and *B*) Developing FB-MO complexes in *dpy-5* (control; *A*) and *spe-4(q347) dpy-5* (*B*) primary spermatocytes. The association of FB's with MO's and the presence of a double layered membrane around the FB observed in controls is not seen in *spe-4*. (*D* and *H*) Division of *spe-4* spermatocytes. Both micrographs depict cells with at least two nuclei (there could be two more nuclei in each of these cells in another section plane). Sometimes more than one nucleus resides in a cell that is not attempting to divide (D; *q347*) and other times the cell is obviously constricted (H; *hc81*). Note distended MO's that are not associated with FB's; the latter are not membrane bound. Also note the granular "necklace" (*arrowheads*) surrounding the nuclei, and vacuoles (*V*) that are not observed in wild type and are presumed to be MO-derived in *D*. (*G*) Higher magnification view of an example of abnormal MO's in *spe-4(q347)* terminal spermatocytes. (*C*) Control spermatids budding from the residual body (not evident in this section plane) in which the FB's are still at least partly membrane bound and (*F*) after completion of budding and completion of FB disassembly. Note the prominent MO's near the cell surface. (*E*) Region of a spermatozoon showing a MO that has fused with the cell surface. A permanent fusion pore (*arrow*) is evident. Bars: (*A–D*, *F*, and *H*) 1 μm; (*E* and *G*) 0.5 μm.

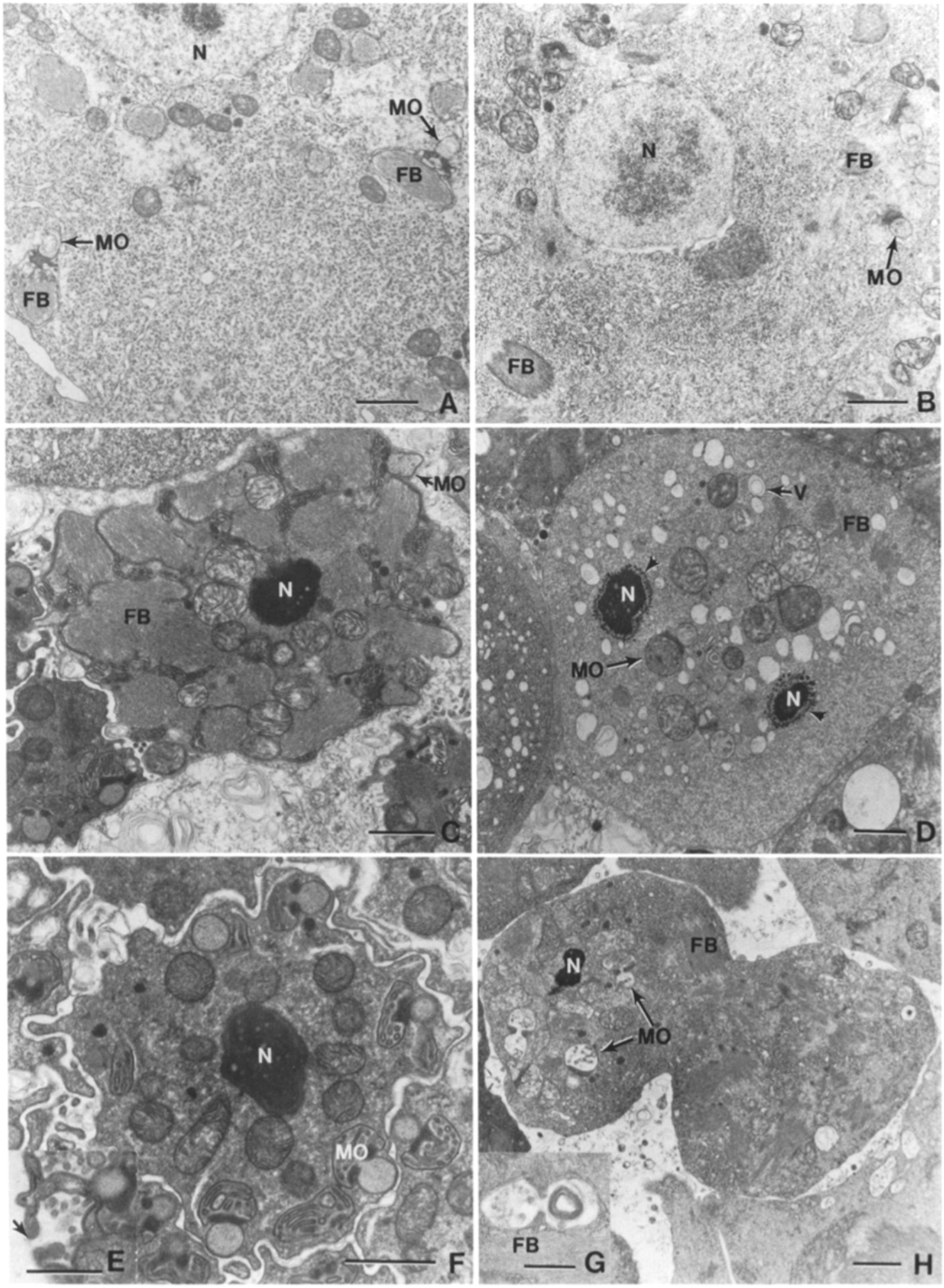
N
MO
FB
MO
FB
A
N
FB
MO
FB
B
MO
N
FB
C
V
FB
N
MO
N
D
N
MO
E
F
FB
N
MO
FB
G
H

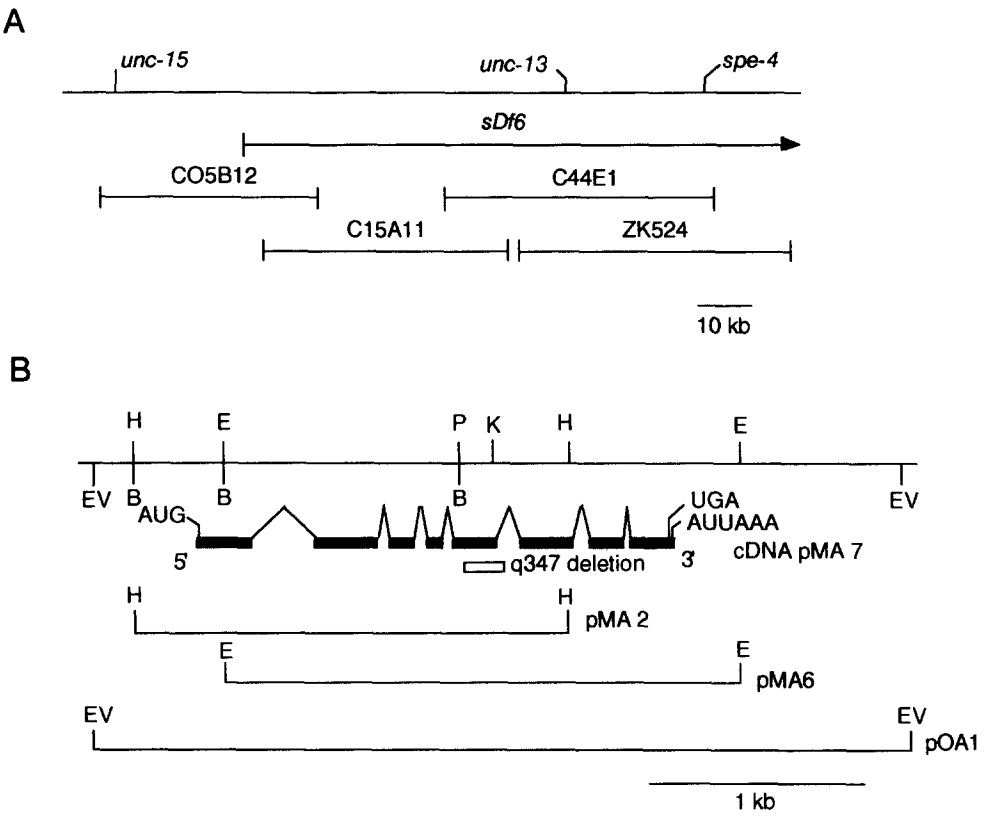

Figure 4. Genetic and physical maps of the *spe-4* region. (*A*) The position of *spe-4* relative to other nearby genes is shown at the top of the figure. The position of *spe-4* was determined by combined genetic and molecular techniques. The corresponding *C. elegans* physical map is shown at the bottom of the figure, and each horizontal line represents a cosmid (the construction and analysis of the physical map is explained in Coulson et al., 1986). The molecular localization of the left breakpoint of *sDf6* was discovered by Maruyama and Brenner (1991) and confirmed during this study (data not shown). The *spe-4* gene lies near the right end of the C44E1 insert (see Results). (*B*) Restriction map of the *spe-4* region deduced from genomic DNA. The lines under the map are cDNA (pMA7) or cloned, genomic restriction fragments that were sequenced (pMA2 and pMA6) or used for transgenic rescue (pOA1). The exons, as found in cDNA pMA7 and primer extension, appear as thick boxes while introns are the thin lines connecting the boxes. *B*, BamHI; *E*, EcoRI; EV, EcoRV; *H*, HinDIII; *K*, KpnI; *P*, PstI.

during meiosis II (Fig. 3 *c*) and the FB's disassemble while the MO's move to the cell surfaces (Fig. 3 *f*). The wild type FB's remain surrounded by a double membrane until the spermatid buds off the residual body (Wolf et al., 1978; Ward et al., 1981; Roberts et al., 1986). The MO's then fuse with the cell surface and undergo exocytosis during formation of the mature spermatozoon (Fig. 3 *e*). We have not observed *spe-4* terminal spermatocytes (Fig. 3, *d*, *g*, and *h*) that contained any MO's like those found in wild-type spermatids (Fig. 3, *c* and *f*) or spermatozoa (Fig. 3 *e*).

Genetics

The *spe-4* gene has been mapped to chromosome I and shown to complement *sDf5* but failed to complement *sDf6* (L'Hernault et al., 1988). This placed *spe-4* near the *unc-15 unc-13* interval, which is <.025 map unit, and to the right of *unc-15* (Rose and Baillie, 1980) (Fig. 4 *a*). We recovered Unc recombinants from *spe-4(hc78)/unc-15(e73) unc-13(e51)* animals and 2/2 *unc-15* animals were Spe while 0/3 *unc-13* animals were Spe, which also suggests that *spe-4* is to the right of *unc-15*. Two factor mapping in *cis* was then performed on *unc-13(e1091)spe-4(q347)*/++. 10 complete broods comprised of 2,951 animals were analyzed; only one of 730 *unc-13* animals was fertile and all 2,221 wild types were fertile. This suggests that *spe-4* is ~0.7 map unit from *unc-13*, based on the previously described two factor mapping equation (Fig. 4 *a*; Brenner, 1974). The correspondence of the genetic map with the physical map can vary in different regions of the *C. elegans* genome (e.g., Greenwald et al., 1987) but in the *unc-15 unc-13* interval, 1 map unit is ~3,200 kb of DNA (Maruyama and Brenner, 1991). This meant that *spe-4* was possibly within 225 kb of *unc-13*.

Molecular Localization of spe-4

The physical map of chromosome I is nearly complete in the region where *spe-4* is located (Coulson et al., 1986, 1988), and we obtained a number of cosmid clones that are located in this region. Genomic DNA was prepared from *C. elegans* strains heterozygous for one of the three *spe-4* alleles, transferred to Southern blots, and probed with several recombinant cosmids containing a portion of chromosome I in order to search for a RFLP. Two of these cosmids, C44E1 (Fig. 4 *a*) and ZK524 (data not shown), identified a RFLP associated with the spontaneous *spe-4* allele *q347* (Fig. 5 *a*); these two cosmids are partially overlapping. RFLP's associated with *q347* were also observed when genomic DNA was digested with any of five other restriction enzymes, and a restriction map of the *spe-4* region is shown in Fig. 4 *b*. In all cases, this RFLP appeared to be a deletion of about 150–200 bp (see below). Genomic DNA from a recombinant non-Spe *unc-13* strain recovered from *unc-13(e1091) spe-4(q347)*/++ heterozygotes (see Genetics section above) lacked this RFLP indicating that the *q347* deletion and Spe phenotype co-segregate (data not shown). Three wild type restriction fragments from this region that appeared affected by the *q347* mutation were subcloned from the cosmid

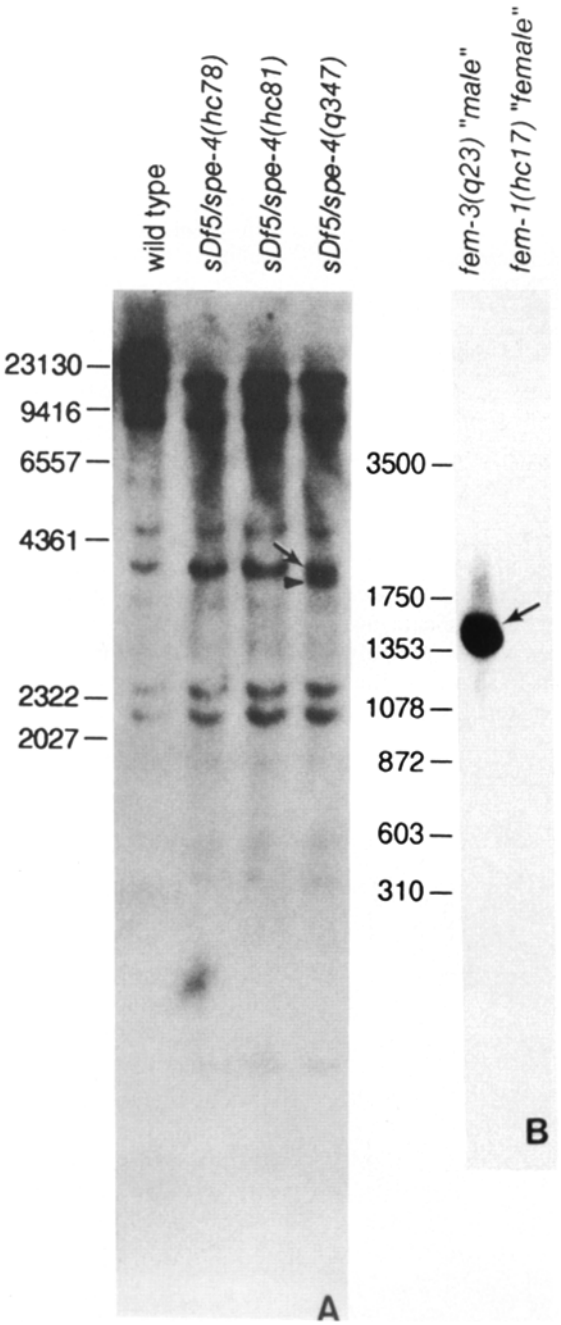

Figure 5. (*A*) DNA polymorphisms in *spe-4*. DNA was prepared from wild type N2 and the heterozygous balanced *spe-4* strains *sDf5/spe-4(hc78)*, *sDf5/spe-4(hc81)*, and *sDf5/spe-4(q347)*. 5 μg of DNA was digested with EcoRV, subjected to electrophoresis in a 0.7% agarose gel, transferred onto Hybond N, and hybridized to ^{32}P-labeled cosmid C44E1. The arrowhead indicates the polymorphic restriction fragment associated with *spe-4(q347)*. The arrow indicates the corresponding wild type restriction fragment. (*B*) Northern hybridization with a *spe-4* specific probe. Total RNA was prepared from *fem-1(hc17)* or *fem-3(q23)* worms reared at 25°C. Under these growth conditions, both of these mutant strains have female somatic tissues but the germline of *fem-1(hc17)* contains oocytes, but no sperm, while the germline of *fem-3(q23)* contains sperm but no oocytes. 20 μg of total RNA was subjected to electrophoresis in a 1.4% agarose gel containing formaldehyde, transferred to nylon and hybridized to the *spe-4* genomic clone pMA2 (see Fig. 4 for the position of pMA2). The probe detects one ~1.5-kb spermatogenesis specific RNA. The sex nonspecific 5.9-kb mRNA encoded by *unc-13* (Maruyama and Brenner, 1991) is present in these *fem-1* and *fem-3* RNA samples and has been detected with *unc-13* specific probes (data not shown). For both *A* and *B*, size standards are indicated along the left margin of each figure.

C44E1 (pMA2 and pMA6) or ZK524 (pOA1; Fig. 4 *b*). These three recombinant plasmids were used as probes, DNA sequencing templates, and/or constructs for creation of transgenic worms, as described below. The right breakpoint of cosmid C44E1 lies between the rightmost EcoRI and EcoRV restriction sites depicted in Fig. 4 *b* (data not shown). This places the *spe-4* gene at the right end of the C44E1 recombinant insert and to the right of *unc-13*, which begins closer to the other end of this cosmid (Maruyama and Brenner, 1991). Both *unc-13* and *spe-4* are transcribed left to right, and a near full length *unc-13* cDNA does not hybridize to either pMA2 or pMA6 (data not shown).

The ultrastructural phenotype of *spe-4* mutants suggests that a polypeptide within sperm might be affected by mutation of this gene. These data suggest that *spe-4* transcription might occur only within animals engaged in spermatogenesis. This was examined by performing Northern hybridizations to blots containing RNA from worms that either contained sperm (genotype: *fem-3[q23gf]* raised at 25°C) or lacked sperm (genotype: *fem-1[hc17ts]* raised at 25°C). An ~1.5-kb RNA was found only in *fem-3* RNA when this blot was probed with a wild type 1.8-kb restriction fragment that included the region affected by the *q347* deletion (pMA2, see Fig. 4 *b* for its position). Both *fem-1(hc17)* and *fem-3(q23)* have female somatic tissues and, since they differ only in their germline, this suggests that pMA2 contains part of a gene that is spermatogenesis or sperm specific (Fig. 5 *b*). Complementary DNA clones corresponding to the ~1.5-kb RNA were isolated by screening *C. elegans* libraries with a pMA2 insert probe. Insert size and Southern hybridization experiments (data not shown) indicated that the largest cDNA, pMA7, was near full length (see below), and within a region encompassed by subclones pMA2 and pMA6 (Fig. 4 *b*).

The above-mentioned genetic and molecular data all are consistent with a *spe-4* location near and to the right of *unc-13* on chromosome I. We sought to confirm the location of *spe-4* by microinjecting worms with a recombinant plasmid that contained DNA from the presumed *spe-4* region. A total of 34 *gld-1/lunc-13 spe-4 lin-10* heterozygous hermaphrodites were microinjected with the recombinant plasmid pOA1 (for the position of pOA1, see Fig. 4 *b*); 18 of these 34 hermaphrodites were co-injected with the *rol-6* plasmid pRF4 as a dominant behavioral marker (see Materials and Methods). Fertility was restored to *spe-4* worms microinjected with pOA1, and the results of these experiments are summarized in Table II. The pOA1 plasmid contains a 3.8-kb EcoRV restriction fragment that includes the entire putative *spe-4* transcription unit, ~450 bp 5′ to the transcription start and ~1,200 bp 3′ to the proposed polyadenylation signal (see below). Three independently derived stable transformed lines were created and, in one case, a transgenic line (*ebEx3*) was outcrossed to replace both *unc-13 spe-4 lin-10* chromosomes with *spe-4* chromosomes. This outcross was performed in order to eliminate the *lin-10* gene because its vulvaless phenotype results in broods that are much smaller than non-

Table II. Characterization of Three spe-4 Transgenes

Transgene	Chromosome I genotype	Germline inheritance of transgene	Brood size (mean ± SD)
–	*unc-13 spe-4 lin-10*	–	0 (n = 45)
ebEx1	*unc-13 spe-4 lin-10*	19 of 70 were fertile	13 ± 7 (n = 21)
ebEx2	*unc-13 spe-4 lin-10*	33 of 58 were fertile	20 ± 8 (n = 20)
ebEx3	*unc-13 spe-4 lin-10*	ND	28 ± 9 (n = 12)
–	*unc-13 + lin-10*	–	27 ± 13 (n = 10)
ebEx3	+ *spe-4* +	103 of 128 were fertile*	169 ± 50 (n = 12)
ebEx3	+ + +	ND	212 ± 48 (n = 11)

Stable transgenic strains bearing the extrachromosomal arrays *ebEx1*, *ebEx2*, or *ebEx3* were recovered from *unc-13(e1091) spe-4(q347) lin-10(e1439)I* hermaphrodites that were microinjected with plasmid DNA. Inheritance of these transgenes and the brood sizes of transgenic hermaphrodites were compared to non-transgenic control strains. These transgenes all contain the *spe-4* plasmid pOA1, and *ebEx2* and *ebEx3* also contain the *rol-6(su1006)II* plasmid pRF4 dominant selectable marker (see Materials and Methods). Brood sizes were determined for the bracketed number of hermaphrodites (n) and are presented as the mean number of progeny with the standard deviation (SD). *ebEx3* was crossed into a *spe-4(q347)* or wild type chromosome I background in order to examine the brood size of non-Lin non-Unc hermaphrodites carrying this transgene.

* ~6% of the worms that inherit *ebEx3* are mosaics that are either sterile rollers, fertile non-rollers, or express the rolling phenotype in only a portion of their cuticle.

ND, not determined.

Lin hermaphrodites (Table II). Construction of this strain relied on following the dominant rolling phenotype associated with transgenes that include a *rol-6(su1004)II* mutant plasmid, such as *ebEx3* (Mello et al., 1991). The continued presence of *spe-4* wild type sequence within the *ebEx3* transgene following this cross was directly demonstrated by PCR in which an amplified product formed only when *spe-4* sequences were continuous with at least a portion of the Bluescript cloning vector (Fig. 6). The resulting *ebEx3/spe-4* hermaphrodites had an average brood size that was ~81% of *ebEx3*/+ non-*spe-4* controls (Table II). Detailed examination of the progeny of *ebEx3/spe-4* hermaphrodites indicated that this transgene behaves like an extrachromosomal array that is mitotically unstable (Table II), which could explain why *ebEx3/spe-4* did not have a wild type brood size. Consequently, it appears that pOA1 contains most, or perhaps all, sequence information required to restore fertility to *spe-4* hermaphrodites.

Sequence of the spe-4 Gene

We determined the sequence of cDNA pMA7 on the sense strand and the corresponding, as well as flanking, genomic region on both strands (Fig. 7). Comparison of the genomic and cDNA sequences reveals that the *spe-4* gene is composed of eight exons, and that pMA7 has a 10 nucleotide polyA tail at its 3′ end. The polyA tail is preceded by an imperfect match to the AATAAA consensus polyadenylation signal (Proudfoot and Brownlee, 1976). Primer extension indicates that the 5′ end of the *spe-4* transcript is 23 nucleotides longer than cDNA pMA7 (Fig. 8 *a*). This experiment predicts that the 5′ end of the *spe-4* transcript is at position 1 (Fig. 7), assuming no additional intron splicing. A sense primer (primer #1, Table I) at this presumed 5′ end was then used to show that it could prime PCR sense strand products following reverse transcription PCR with an antisense primer (primer #3, see Table I). The resulting product of this PCR closely corresponds in size to the predicted 236-bp fragment (Fig. 8 *b*), indicating that nucleotides 1–23 of the genomic sequence are found in the *spe-4* mRNA and are not interrupted by an intron. Furthermore, both primer extension and reverse transcription PCR confirm that the transcription of *spe-4* occurs only in animals engaged in spermatogenesis.

The data discussed above establish the transcription initiation point and indicate that the *spe-4* transcript is 1,484 nucleotides without the polyA 3′ tail (Fig. 7). The first ATG at position 16 shows excellent agreement with the consensus translation start for *C. elegans* (Perry, M. D., G. H. Hertz,

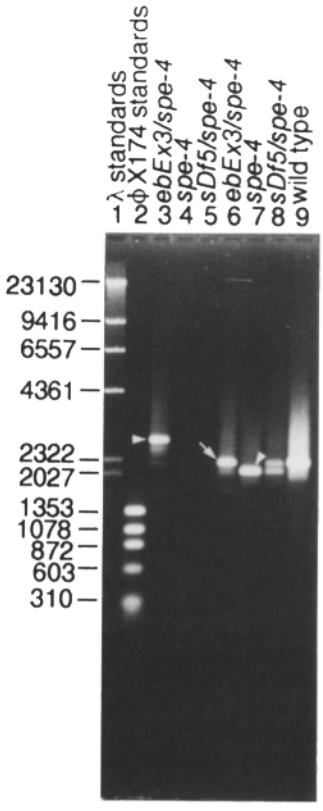

Figure 6. PCR of an *ebEx3* bearing transgenic strain. Individual worms that were either *ebEx3/spe-4(q347)*, *spe-4(q347)*, *sDf5/spe-4(q347)*, or wild type N2 were pooled by genotype, DNA was prepared, and aliquots derived from the equivalent of eight worms were subjected to PCR. Each lane of this ethidium bromide stained 0.7% agarose gel contains eight percent of the resulting PCR products. The primer pair was #1 and #7 for lanes *3–5*, and only the transgene bearing strain shows the expected ~3.0-kb band (*arrowhead*, lane *3*) associated with an intact *spe-4* gene in Bluescript (see Table I for the position of PCR primers). The primer pair was #1 and #6 for lanes *6–9*, and the size of these PCR products confirms the genotypes of the DNA samples and indicates that the chromosome I copies of the mutant and wild type *spe-4* gene are intact and can function as PCR templates. Strains with a non-*spe-4(q347)* chromosome I (or a transgene containing wild-type *spe-4*) show the expected ~2.5-kb amplification product (*arrow*, lane *6*; note that this band is also present in lanes *8* and *9*) while strains containing a *spe-4(q347)* chromosome I show the expected ~2.3-kb amplification product (*arrowhead*, lane *7*; note that this band is also present in lane *8*). The size of molecular weight standards appear along the left margin of the figure.

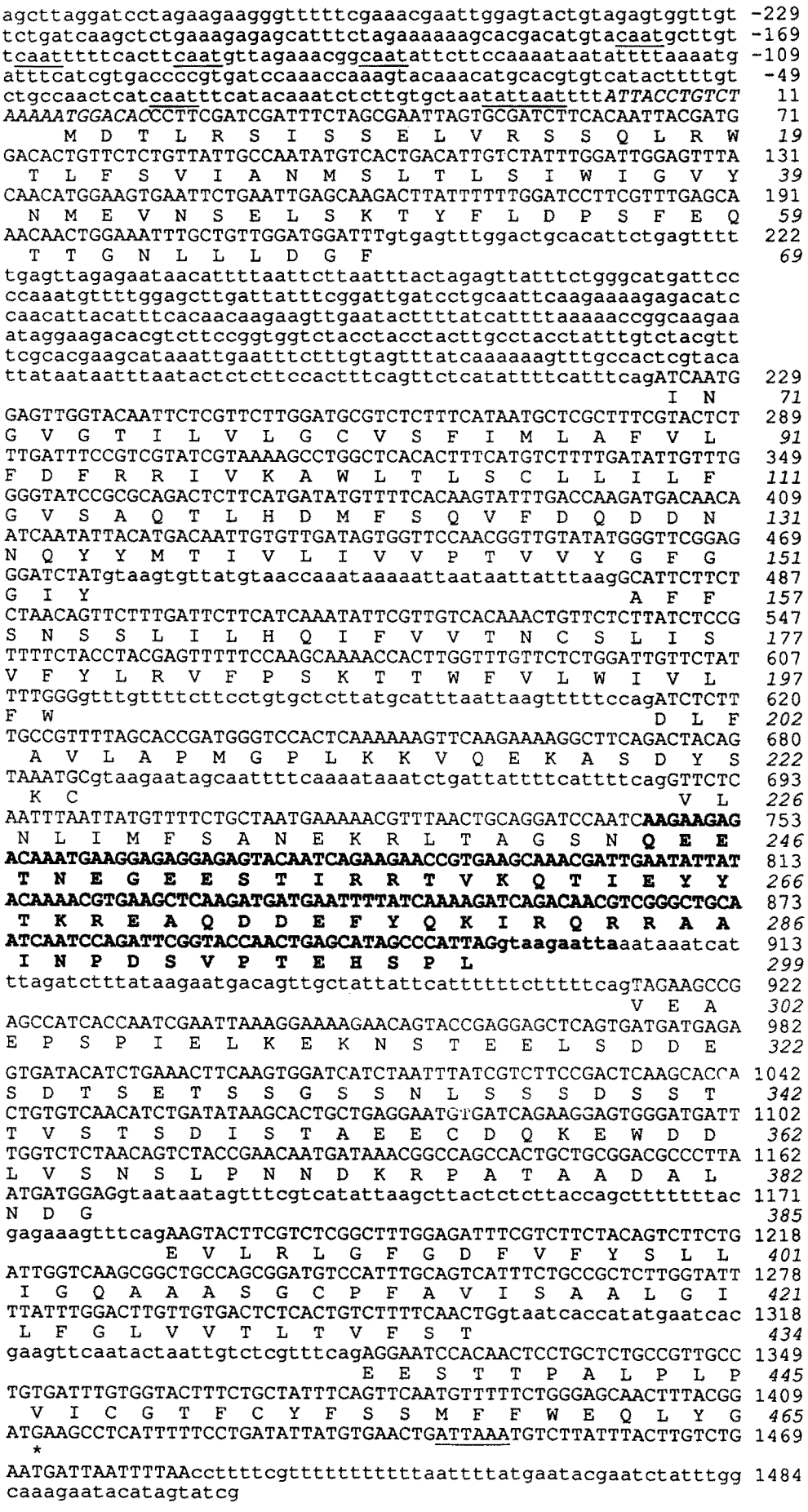

Figure 7. Sequence of the *spe-4* gene and flanking regions. A total of 2,539 nucleotides of genomic sequence are shown with the deduced amino acid sequence appearing below the line in one-letter code. The transcription start, based on primer extension, is indicated by +1. The proposed initiator methionine begins at position +16 and the termination codon begins at position 1,411. cDNA sequence appears in upper case, non-italicized letters, introns and flanking regions appear in lower case. The positive numbers at the right are nucleotide positions from the sequence of cDNA pMA7 and primer extension; the 5′23 nucleotides are upper case and italicized to reflect the fact that they have been determined by primer extension of either *him-5* males or 25°C grown *fem-3* RNA; they are not templated from 25°C grown *fem-1* RNA. The nucleotides in the genomic sequence that are 5′ to the 5′ end of the primer extension product are negatively numbered and in lower case, and nucleotides within introns and in the 3′ flanking region are in lower case and not numbered. Italicized numbers on the right refer to amino acid residues. A potential TATA box and CAAT sequences at the 5′ end of the gene and a potential polyadenylation signal sequence at the 3′ end of the gene are all underlined. The 178 nucleotides of sequence, and the corresponding amino acid residues, deleted by the *spe-4(q347)* mutation appear in bold. These sequence data are available from EMBL/GenBank/DDBJ under accession number Z14066 for the cDNA and Z14067 for the genomic sequence.

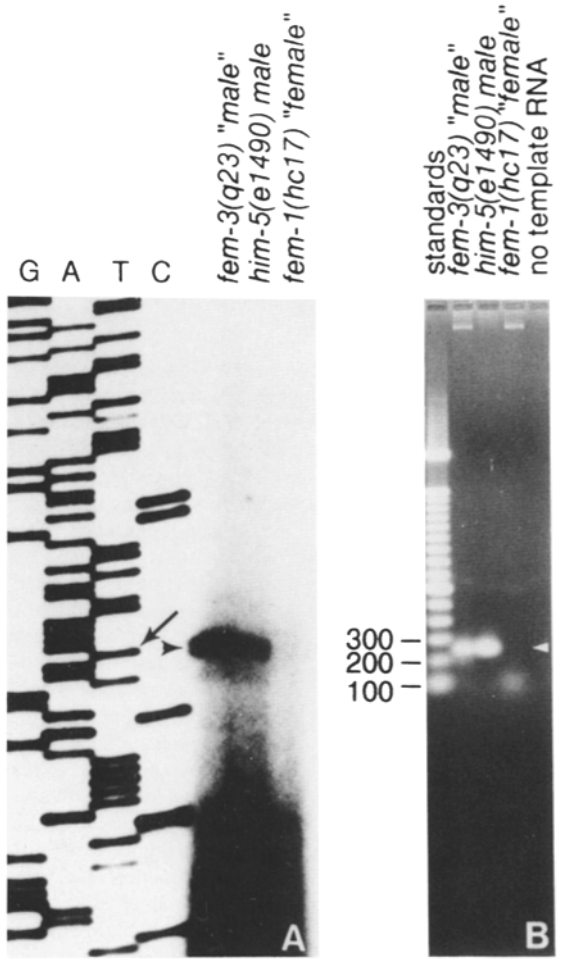

Figure 8. Primer extension and reverse transcription PCR of *spe-4* transcripts. For both techniques, the template total RNA was either *fem-3* (which has a female soma and makes sperm but not oocytes), *him-5* males (male soma and germline) or, as a negative control, *fem-1* (female soma and germline). (*a*) Identification of the 5′ end of the *spe-4* transcript by primer extension. The three rightmost lanes contain the products of a primer extension reaction using a ^{32}P end-labeled oligonucleotide (primer #2, see Table I) hybridized to 20 μg of total RNA. The size of the DNA products of reverse transcription was determined by comparison to DNA sequencing reactions primed with primer #2 and shown in the four leftmost lanes. These primer extension results indicate that the 5′ end is an *A* (the sense strand complement of the *T* at the arrow), which is position +1 in Fig. 7. Note that both *fem-3* and *him-5* (which have sperm) form products (*arrowheads*) while no product is formed from *fem-1* females (which lack sperm). (*b*) Confirmation of the 5′ end of the *spe-4* transcript by reverse transcription PCR. Reverse transcription was performed on 250 ng of total RNA hybridized to primer #3. Primer #1, designed to be at the 5′ transcription start as determined by primer extension (see Fig. 8 *a*), was then added, PCR was performed, and the three rightmost lanes of this ethidium bromide stained 1.5% agarose gel contain 5% of the products of these reactions. Note that both *fem-3* and *him-5* (which have sperm) form the expected 236-bp product (*arrowhead*) while no product is formed from *fem-1* females (which lack sperm). The size standards for *b* are a 100-bp DNA ladder, and the positions of the 100-, 200-, and 300-bp fragments appear along the left margin of the figure.

and W. B. Wood, personal communication) and, if one assumes that it is used, the predicted polypeptide is 465 amino acids. The *spe-4* gene contains seven introns and six of these are short (42–71 nucleotides) as is typical for *C. elegans* genes (Blumenthal and Thomas, 1988). The open reading frame (ORF) defined by cDNA pMA7 and primer extension extends to the 5′ end of the transcript and shows excellent agreement to a *C. elegans* codon usage table provided by C. Fields (personal communication; Fig. 9).

Restriction mapping and sequencing of the cDNA pMA7 suggested that the deletion present in *spe-4(q347)* probably affected the *spe-4* encoded protein. Additional restriction mapping revealed that exon five contained a KpnI site that was lacking in *spe-4(q347)* (Fig. 10 *a*). PCR primers were

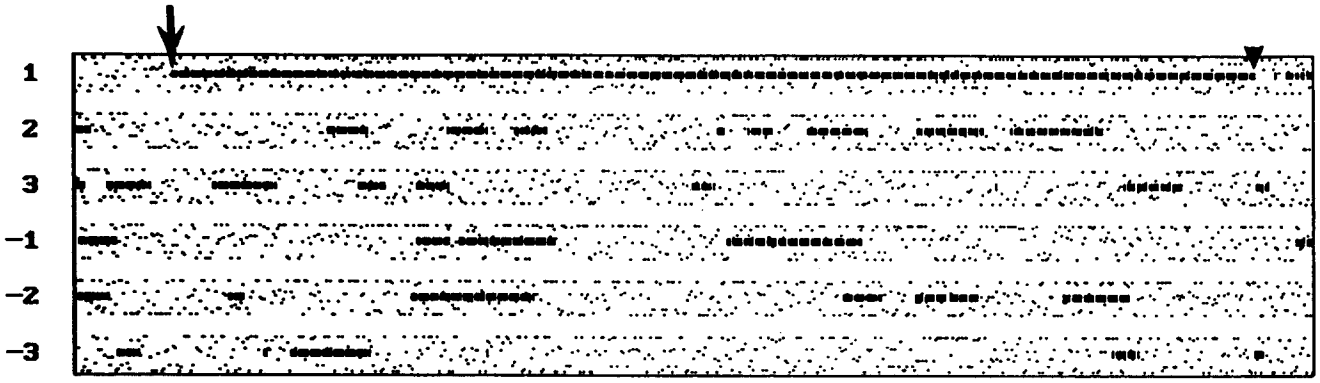

Figure 9. Analysis of ORFs within the pMA7 cDNA sequence and the ORF that extends from the 5′ end of pMA7 to position -108 in the genomic sequence (see Fig. 7). All six potential reading frames are displayed by the GENEPRO program (Riverside Scientific), which can evaluate the codon usage within ORFs. Any potential ORFs that start with a methionine are indicated by a thick dashed horizontal bar. Superimposed on the horizontal bars are a series of dots. Each dot represents a comparison of the codon used at that position in the ORF and a table of codon usage provided by C. Fields (Institute for Genomic Research, Gaithersburg, MD). The vertical position of dots relative to the horizontal dashed bar indicates similarity to the *C. elegans* codon usage table. Dots above the bar are more similar to the table values than dots below the bar. The ORF in reading frame one (indicated on the ordinate) is open to the left border of the plot and the first ATG methionine codon (the start of the thick, dashed bar) is the proposed translational start. This ATG (*arrow*; also see position 16 in Fig. 7) is followed by a single long ORF (1395 nucleotides, 465 amino acid residues) that shows excellent agreement with *C. elegans* codon usage (note the large number of dots above the thick, dashed line). This ORF terminates in a TGA stop codon (at arrowhead; also see position 1,411 in Fig. 7).

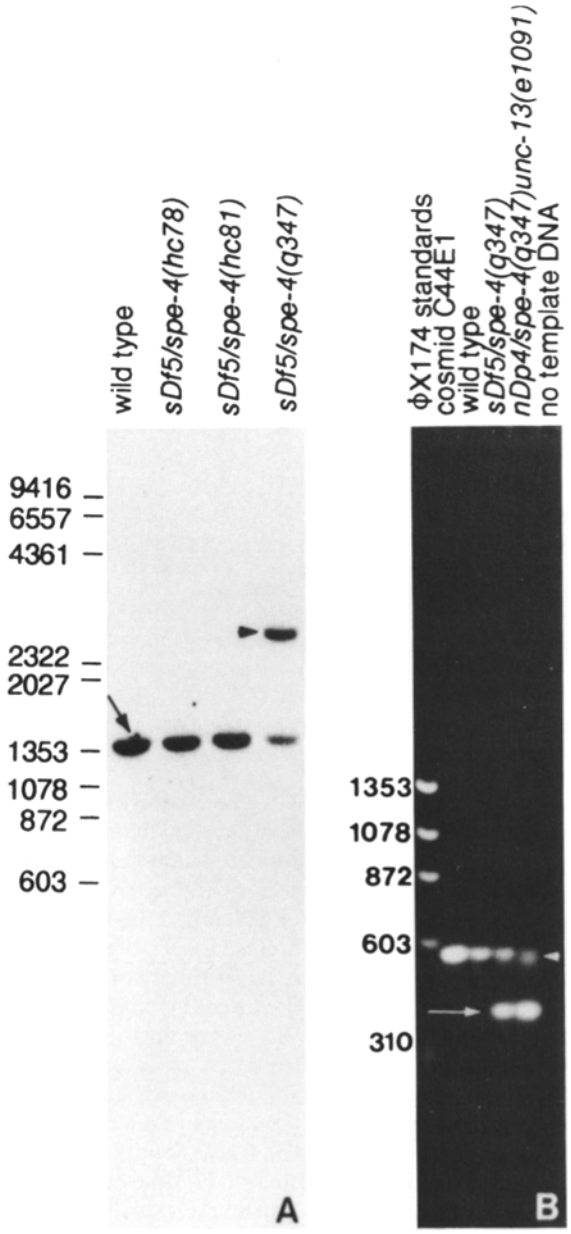

Figure 10. Further characterization of the genomic region affected by *spe-4(q347)*. (*A*) 5 μg of genomic DNA from N2(wild-type), *sDf5/spe-4(hc78)*, *sDf5/spe-4(hc81)*, or *sDf5/spe-4(q347)* was double-digested with EcoRI and KpnI and subjected to electrophoresis on a 1% agarose gel, transferred to nylon, and hybridized to an oligolabeled large EcoRI insert fragment of the cDNA pMA7. The probe is homologous to two EcoRI/KpnI restriction fragments that are both ~1.3 kb (*arrow*). Deletion of the single KpnI site between these two EcoRI sites by the *spe-4(q347)* mutation results in a fusion fragment of ~2.4 kb (*arrowhead*). (*B*) PCR strategy to obtain the sequence of the region deleted by the *spe-4(q347)* mutation. PCR was performed as described in Materials and Methods. The PCR primers were #4 and #5 (see Table I). An ethidium bromide stained 1.5% agarose gel that had been loaded with 10% of the PCR products of 1 ng C44E1 recombinant cosmid DNA, 100 ng genomic DNA, or a "no added template" DNA control is shown. The cosmid and all samples of *C. elegans* genomic DNA produced the wild type product (*arrowhead*) while strains containing *spe-4(q347)*, in addition, produced a smaller fragment (*arrow*). We used two different heterozygous *spe-4(q347)* strains in order to ensure that the balancer chromosome (*sDf5* or *nDp4*) was not the template for this smaller fragment (*arrow*). For both *A* and *B*, size standards are indicated along the left margin of each figure.

then designed to allow amplification of DNA flanking the region that was deleted in this mutant. These primers (primers #4 and 5, see Table I) should produce a *spe-4*–derived PCR product of 558 bp from wild type genomic DNA and a product that is 150–200 bp smaller than wild-type when *q347* genomic DNA was used as the template; these predictions are in close agreement with what was observed (Fig. 10 *b*). The amplified PCR product associated with the *q347* deletion was sequenced, and the 178 bp of the *spe-4* gene that are deleted by the *q347* mutation are shown in bold in Fig. 7.

The position of the *spe-4(q347)* deletion indicates that the structure of the *spe-4* protein will be affected by this mutation. The *q347* deletion removes part of both exon 5 and intron 5, including the splice donor sequence between this exon and intron (Fig. 4 *b*). Unless a cryptic splice donor is present, the *q347* deletion will shift the reading frame and add one amino acid now capable of being encoded by intron 5 (and not found in wild type *spe-4* protein) followed by a TAA stop codon in intron 5. Assuming that the *q347* mRNA is translated, a polypeptide of 244 amino acids rather than the wild type 465 amino acids would result.

A hydropathy plot (Kyte and Doolittle, 1982) of the *spe-4* protein indicates that it is likely to be an integral membrane protein (Fig. 11). There are at least seven regions that could span the membrane using the conservative window of 19 residues and the first, third, and sixth regions are followed by a sequence of charged residues. As compared with other membrane proteins, the deduced amino acid sequence near the NH_2 terminus and the position of the first proposed membrane spanning region suggests that the *spe-4* polypeptide lacks a cleavable NH_2 terminal signal sequence (von Heijne, 1985). The region from residues 211–394 is hydrophilic, as it contains many charged and polar residues, and presumably faces either the extracellular space or the lumen of a vesicle. There are a total of five potential N-linked glycosylation sites in the *spe-4* protein at positions 27, 159, 172, 313, and 334; we do not know if these sites are used but the last two are located within the above-mentioned hydrophilic region (Fig. 11). The *spe-4* protein has no significant homology to other proteins in either the GENPEPT (update 71) or SWISS-PROT (update 21) databases. The most significant matches were to membrane spanning domains within several other integral membrane proteins (data not shown).

Discussion

We have presented phenotypic, genetic, and molecular analyses of *spe-4*, a gene involved in sperm morphogenesis. We have discovered that the genetic lesion within a spontaneous allele is a small deletion and, after localizing this deletion on the physical map of chromosome I, have cloned the *spe-4* gene. This cloned DNA can rescue *spe-4* associated sterility in germline transformation experiments. Transcription of the *spe-4* gene results in an ~1.5-kb polyA+ mRNA that is produced only in animals engaged in spermatogenesis. This *spe-4* mRNA encodes a protein that is not homologous to

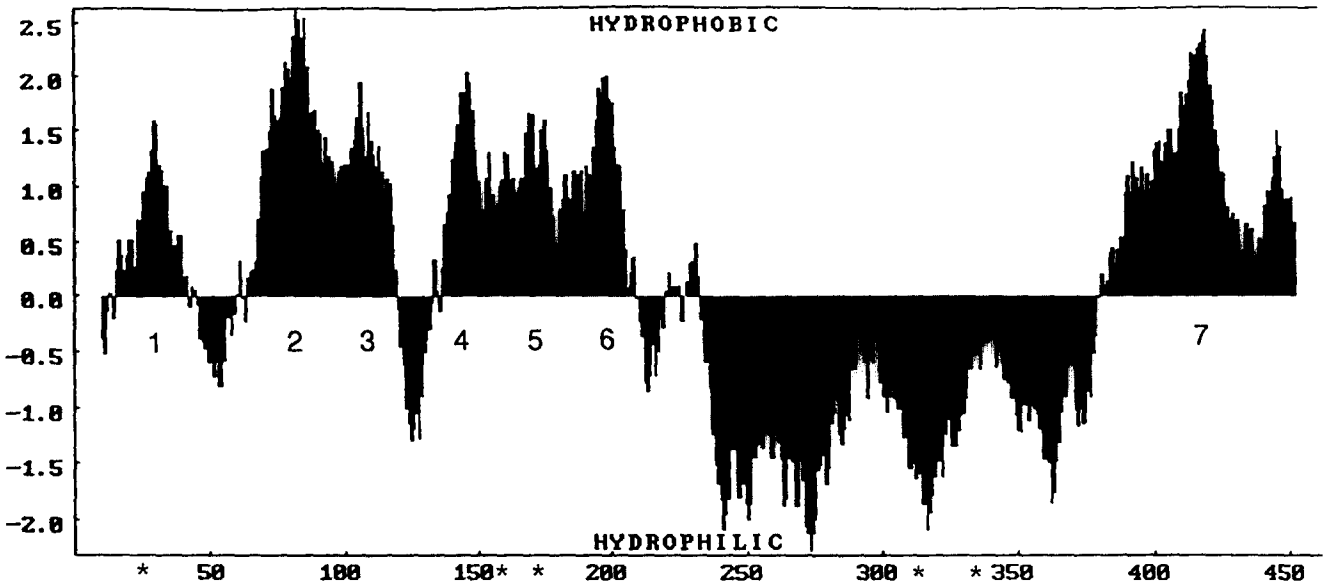

Figure 11. Hydropathy plot of *spe-4* protein. The algorithm of Kyte and Doolittle (1982), as implemented under the GENEPRO program, was used. The window was set to nineteen residues for this plot. Potential membrane spanning regions are numbered under the peak of hydropathy and numbering starts from the NH_2 terminus. Five potential N-linked glycosylation sites are indicated below the abscissa by an asterisk.

previously characterized proteins, but hydropathy analysis indicates that it is probably an integral transmembrane protein that passes through the lipid bilayer multiple times.

The sterile phenotype of *spe-4* mutants is caused by their failure to form normal spermatids and, consequently, functional spermatozoa. All three *spe-4* alleles are completely penetrant for this sterile phenotype and form terminal spermatocytes in which meiotic nuclear divisions have occurred without the usually concomitant cell divisions. The major subcellular defect revealed by ultrastructural analyses of *spe-4* mutant spermatocytes is disruption of the FB-MO complexes. These structures, which are first observed in spermatocytes prior to the first meiotic division, apparently play a role that is unique to nematode sperm. Unlike flagellated sperm, where spermatids contain ribosomes engaged in translation and a lengthy time interval separates the second meiotic division from loss of ribosomes to the residual body (for review see Olds-Clarke, 1988), nematode spermatids do not contain ribosomes because they are discarded into the residual body as these cells form (Wolf et al., 1978; Ward et al., 1981). Consequently, all protein components that are necessary for subsequent differentiation into spermatozoa must be placed within the spermatid as it forms. The FB-MO complexes ensure that macromolecules synthesized in spermatocytes are segregated to spermatids during the cytokinesis that accompanies the second meiotic division. Components within the FB-MO complexes include proteins that are necessary for differentiation of spermatozoa (Ward and Klass, 1982; Roberts et al., 1986).

Ultrastructural localization of gold-conjugated mAbs specific for sperm antigens has been used to elucidate many details of how FB-MO complexes form during *C. elegans* spermatogenesis (Roberts et al., 1986). One of these antibodies recognizes MSP, and it localizes to the fibers that are within the FB. A second antibody (Ward et al., 1986) recognizes proteins within membranes of the FB-MO's and the sperm plasma membrane. These studies reveal that MO's appear prior to the FB's, and each FB forms in close association with an MO and becomes surrounded by MO-derived membrane as it grows by adding new MSP containing fibers. In contrast, our work suggests that a close association of FB's with MO's does not occur in either *spe-4* primary or terminal spermatocytes. It has been suggested that the wild type FB represents a membrane enclosed site where fibers can form because the localized high concentration of soluble MSP favors polymer (=fiber) formation. Our work has established that fiber integrity in *spe-4* mutants requires neither continuous association of an FB with a MO nor the presence of a surrounding membrane. Detailed study of the early morphogenesis of FB's in *spe-4* mutants should reveal how FB's form and if there is ever association of MO's with FB's.

FB-MO complexes contain several proteins that are required by the *C. elegans* spermatozoon, and they are segregated to the spermatid during meiosis II when this cell separates from the residual body. The membrane around each FB retracts towards its associated MO, the fibers of the FB disassemble, releasing their MSP contents to the cytoplasm (Ward and Klass, 1982; Roberts et al., 1986) and the MO moves to the cell surface. The MO then fuses with the cell surface and forms a permanent fusion pore as it releases its contents onto the cell surface by exocytosis during conversion of spermatids to spermatozoa (Wolf et al., 1978; Nelson and Ward, 1980; Ward et al., 1981). MSP localizes within the pseudopod where it appears to play a cytoskeletal role (Roberts, 1983; Roberts et al., 1989; Sepsenwol et al., 1989). Unfortunately, it is presently not possible to determine whether the *spe-4* protein functions in gametes because mutations in this gene arrest cellular morphogenesis prior to spermatid formation. Recovery of appropriate temperature sensitive *spe-4* mutations might allow spermatids to form

under permissive conditions. These spermatids could then be shifted to restrictive conditions in order to mutationally disrupt the *spe-4* protein and examine its role within spermatids and during the conversion of spermatids into spermatozoa.

Several genes that affect FB-MO ultrastructure have been identified (e.g., Ward et al., 1981; J. Varkey and S. Ward, personal communication), and one of these genes (*spe-10*) causes a mutant phenotype that shares similarities with some of the *spe-4*–associated defects (Shakes and Ward, 1989*b*). In *spe-10* mutants, each MO prematurely retracts the double membrane that surrounds its associated FB just before or as spermatids are forming; normally, an FB does not lose its association with an MO until after spermatid formation. These FB's do not disassemble their fibrous contents and they end up in the residual body, rather than the spermatid. The MO's are segregated to the spermatid where, instead of developing the compact mushroom-like morphology that is characteristic of wild type MO's, they become large and vacuolated. The MO's within *spe-10* spermatids and the stable FB's that lack surrounding membranes are both similar in appearance to the MO's and FB's observed within *spe-4* terminal spermatocytes. The mutant phenotypes of *spe-4* and *spe-10* both suggest that fibers within an FB that lacks a surrounding membrane only disassemble when they are within spermatids. Additionally, in both *spe-10* and *spe-4*, the MO's are separate from the FB's at the point when they become swollen and abnormal in appearance.

Previous results had indicated that the phenotypic effects of *spe-4* were probably limited to the disruption of spermatogenesis (L'Hernault et al., 1988). This study has revealed that the *spe-4* gene encodes an ~1.5-kb mRNA that is expressed during spermatogenesis. Furthermore, the cloning and sequencing of *spe-4* and a deletion mutation within this gene (*q347*) indicate that the probable *spe-4* null phenotype is limited to disruption of spermatogenesis. Analysis of the *spe-4* sequence suggests that it encodes an integral membrane protein of 465 amino acids. This inference is based on hydropathy plots (Kyte and Doolittle, 1982) that indicate the *spe-4* protein spans the membrane several times. We have used this algorithm at a window of 19 residues for our sequence analyses. A window of this size empirically has been found to permit one to distinguish between hydrophobic regions that span the membrane and those that are located within interior regions of globular proteins. If the average hydropathy of a region is greater than 1.6, this region probably spans a membrane (Kyte and Doolittle, 1982); the *spe-4* protein has at least seven regions that meet this criterion. Integral membrane proteins are synthesized on rough endoplasmic reticulum and usually have a signal sequence that permits their passage into the ER membrane (reviewed by Singer, 1990). The proposed signal sequence in the *spe-4* protein does not appear to be cleavable because it is too far from the NH_2 terminus and lacks the appropriate distribution of charged residues near the putative membrane spanning domain (von Heijne, 1985). Consequently, if this model is correct, the *spe-4* encoded protein should be co-translationally inserted into the endoplasmic reticulum via an internal signal sequence, and the protein should retain its NH_2 terminus after completion of polypeptide synthesis.

Molecular data together with the ultrastructural analyses discussed above suggest *spe-4* encodes an integral membrane protein that resides within membranes that are part of the FB-MO complex. It is also possible that the *spe-4* encoded protein resides within other membranes in sperm. To address this question, we are raising antisera to the *spe-4* encoded protein that has been synthesized in bacteria. Electron microscopic localization of the *spe-4* antigen with specific antibodies should allow unambiguous determination of its subcellular localization in wild type spermatocytes and spermatozoa.

We thank Tim Schedl for providing *spe-4(q347)* and many helpful discussions, Alan Coulson and John Sulston for providing cosmids, Ichi Maruyama for helpful discussions and his restriction map of cosmid C44E1, and Tom Roberts, Barry Yedvobnick, Hilary Ellis, and Guy Benian for their interest and advice. We would also like to thank Nancy L'Hernault, who provided assistance with EM, Ollie Appleberry for technical assistance, and Henry Malter for microinjection advice.

This work was supported by grants from the National Institutes of Health (GM40697) and the Emory University Research Committee to S. W. L'Hernault. Some of the stocks used in this work were obtained from the *Caenorhabditis* Genetics Center, which is supported by a contract grant (1101-AG-9-2113) between the National Institutes of Health and the University of Missouri.

Received for publication 27 January 1992 and in revised form 1 July 1992.

References

Argon, Y., and S. Ward. 1980. *Caenorhabditis elegans* fertilization-defective mutants with abnormal sperm. *Genetics.* 96:413–433.

Ausubel, F. M., R. Brent, R. E. Kingston, D. D. Moore, J. G. Seidman, J. A. Smith, and K. Struhl. 1989. Current Protocols in Molecular Biology. John Wiley and Sons, New York. 482 pp.

Barstead, R. J., and R. H. Waterston. 1991. Vinculin is essential for muscle function in the nematode. *J. Cell Biol.* 114:715–724.

Barton, M. K., T. Schedl, and J. Kimble. 1987. Gain of function mutations of *fem-3*: a sex determination gene in *Caenorhabditis elegans. Genetics.* 115: 107–119.

Blumenthal, T., and J. Thomas. 1988. *Cis* and *trans* mRNA splicing in *Caenorhabditis elegans. Trends Genetics.* 4:305–308.

Brenner, S. 1974. The genetics of *Caenorhabditis elegans. Genetics.* 77:71–94.

Burke, D. J. 1983. A molecular genetic analysis of the major sperm proteins of the nematode *Caenorhabditis elegans.* Ph.D. thesis, Johns Hopkins University. 193 pp.

Burke, D. J., and S. Ward. 1983. Identification of a large multigene family encoding the major sperm protein of *Caenorhabditis elegans. J. Mol. Biol.* 171:1–29.

Church, G. M., and W. Gilbert. 1984. Genomic sequencing. *Proc. Natl. Acad. Sci. USA.* 81:1991–1995.

Collins, J., B. Saari, and P. Anderson. 1987. Activation of a transposable element in the germ line but not the soma of *Caenorhabditis elegans. Nature (Lond.).* 328:726–728.

Coulson, A., J. Sulston, S. Brenner, and J. Karn. 1986. Toward a physical map of the *Caenorhabditis elegans* genome. *Proc. Natl. Acad. Sci. USA.* 83: 7821–7825.

Coulson, A., R. Waterston, J. Kiff, J. Sulston, and Y. Kohara. 1988. Genome linking with artificial chromosomes. *Nature (Lond.).* 335:184–186.

Davidson, E. 1986. Gene Activity in Early Development. Academic Press, New York. 670 pp.

Edgar, L. G. 1982. Control of spermatogenesis in the nematode *Caenorhabditis elegans.* Ph.D. thesis. University of Colorado. 264 pp.

Fire, A. 1986. Integrative transformation of *Caenorhabditis elegans. EMBO (Eur. Mol. Biol. Organ.) J.* 5:2673–2680.

Ferguson, E. L., and H. R. Horvitz. 1985. Identification and characterization of 22 genes that affect the vulval cell lineages of the nematode *Caenorhabditis elegans. Genetics.* 110:17–72.

Greenwald, I., A. Coulson, J. Sulston, and J. Priess. 1987. Correlation of the physical and genetic maps in the *lin-12* region of *Caenorhabditis elegans. Nucleic Acids Res.* 15:2295–2307.

Hirsh, D,. and R. Vanderslice. 1976. Temperature-sensitive developmental mutants of *Caenorhabditis elegans. Dev. Biol.* 49:220–235.

Hodgkin, J., H. R. Horvitz, and S. Brenner. 1979. Nondisjunction mutants of the nematode *Caenorhabditis elegans. Genetics.* 91:67–94.

Horvitz, H. R., S. Brenner, J. Hodgkin, and R. K. Herman. 1979. A uniform genetic nomenclature for the nematode *Caenorhabditis elegans. Mol. Gen. Genet.* 175:129–133.

Innis, M. A., and D. H. Gelfand. 1990. Optimization of PCR. *In* PCR Protocols. M. A. Innis, D. H. Gelfand, J. J. Sninsky, T. J. White, editors. Aca-

demic Press Inc., New York. 3–12.
Kimble, J., and S. Ward. 1988. Germ-line development and fertilization. *In* The Nematode *Caenorhabditis elegans*. W. B. Wood, editor. Cold Spring Harbor, New York. 191–214.
Klass, M. R., and D. Hirsh. 1981. Sperm isolation and biochemical analysis of the major sperm protein from *Caenorhabditis elegans*. *Dev. Biol.* 84:299–312.
Kyte, J., and R. F. Doolittle. 1982. A simple method for displaying the hydropathic character of a protein. *J. Mol. Biol.* 157:105–132.
L'Hernault, S. W., D. C. Shakes, and S. Ward. 1988. Developmental genetics of chromosome I spermatogenesis-defective mutants in the nematode *Caenorhabditis elegans*. *Genetics*. 120:435–452.
Maruyama, I. N., and S. Brenner. 1991. A phorbol ester/diacylglycerol-binding protein encoded by the *unc-13* gene of *Caenorhabditis elegans*. *Proc. Natl. Acad. Sci. USA*. 88:5729–5733.
Mello, C. C., J. M. Kramer, D. Stinchcomb, and V. Ambros. 1991. Efficient gene transfer in *C. elegans*: extrachromosomal maintenance and integration of transforming sequences. *EMBO (Eur. Mol. Biol. Organ.) J.* 10:3959–3970.
Miller, J., D. Ganem, P. Lu, and A. Schmitz. 1977. Genetic studies of the lac repressor I. Correlation of mutational sites with specific amino acid residues: construction of a colinear gene-protein map. *J. Mol. Biol.* 109:275–301.
Nelson, G. A., and S. Ward. 1980. Vesicle fusion, pseudopod extension and amoeboid motility are induced in nematode spermatids by the ionophore monensin. *Cell*. 19:457–464.
Nelson, G. A., K. K. Lew, and S. Ward. 1978. Intersex, a temperature sensitive mutant of the nematode *Caenorhabditis elegans*. *Dev. Biol.* 66:386–409.
Nelson, G. A., T. Roberts, and S. Ward. 1982. *Caenorhabditis elegans* spermatozoan locomotion: amoeboid movement with almost no actin. *J. Cell Biol.* 92:121–131.
Olds-Clarke, P. 1988. Genetic analysis of sperm function in fertilization. *Gam. Res.* 20:241–264.
Pearson, W. R., and D. J. Lipman. 1988. Improved tools for biological sequence comparison. *Proc. Natl. Acad. Sci. USA*. 85:2444–2448.
Proudfoot, N. J., and G. G. Brownlee. 1976. 3′ non-coding region sequences in eucaryotic mRNA. *Nature (Lond.)*. 345:163–167.
Roberts, T. M. 1983. Crawling *Caenorhabditis elegans* spermatozoa contact the substrate only by their pseudopods and contain 2-nm filaments. *Cell Motil.* 3:333–347.
Roberts, T. M., F. M. Pavalko, and S. Ward. 1986. Membrane and cytoplasmic proteins are transported in the same organelle complex during nematode spermatogenesis. *J. Cell Biol.* 102:1787–1796.
Roberts, T. M., S. Sepsenwol, and H. Ris. 1989. Sperm motility in nematodes: crawling movement without actin. *In* The Cell Biology of Fertilization. H. Shatten and G. Schatten, editors. Academic Press, Orlando, FL. 41–60.
Rose, A. M., and D. L. Baile. 1980. Genetic organization of the region around *unc-15*(I), a gene affecting paramyosin in *Caenorhabditis elegans*. *Genetics*. 96:639–648.
Rosenquist, T. A., and J. Kimble. 1988. Molecular cloning and transcript analysis of *fem-3*, a sex-determination gene in *Caenorhabditis elegans*. *Genes Dev.* 2:606–616.
Sambrook, J., E. F. Fritsch, and T. Maniatis. 1989. Molecular Cloning: A Laboratory Manual. 2nd edition. Cold Spring Harbor Laboratory Press, Cold Spring Harbor, New York.
Sanger, F., S. Nicklen, and A. Coulson. 1977. DNA sequencing with chain-terminating inhibitors. *Proc. Natl. Acad. Sci. USA*. 74:5463–5467.
Sepsenwol, S., H. Ris, and T. M. Roberts. 1989. A unique cytoskeleton associated with crawling in the amoeboid sperm of the nematode, *Ascaris suum*. *J. Cell Biol.* 108:55–66.
Shakes, D. C. 1988. A genetic and pharmacological analysis of spermatogenesis in the nematode, *Caenorhabditis elegans* Ph.D. thesis, Johns Hopkins University. 189 pp.
Shakes, D. C., and S. Ward. 1989*a*. Initiation of spermiogenesis in *C. elegans*: a pharmacological and genetic analysis. *Dev. Biol.* 134:189–200.
Shakes, D. C., and S. Ward. 1989*b*. Mutations that disrupt the morphogenesis and localization of a sperm-specific organelle in *Caenorhabditis elegans*. *Dev. Biol.* 134:307–316.
Sigurdson, D. C., G. J. Spanier, and R. K. Herman. 1984. *Caenorhabditis elegans* deficiency mapping. *Genetics*. 108:331–345.
Singer, S. J. 1990. The structure and insertion of integral proteins into membranes. *Ann. Rev. Cell Biol.* 6:247–296.
von Heijne, G. 1985. Signal sequences. The limit of variation. *J. Mol. Biol.* 184:99–105.
Ward, S. 1986. The asymmetric localization of gene products during the development of *Caenorhabditis elegans* spermatozoa. *In* Gametogenesis and the Early Embryo. J. Gall, editor. A. R. Liss, New York. 55–75.
Ward, S., and J. Miwa. 1978. Characterization of a temperature sensitive fertilization-defective mutant of the nematode *Caenorhabditis elegans*. *Genetics*. 88:235–303.
Ward, S., and M. Klass. 1982. The location of the major protein in *C. elegans* sperm and spermatocytes. *Dev. Biol.* 92:203–208.
Ward, S., Y. Argon, and G. A. Nelson. 1981. Sperm morphogenesis in wild-type and fertilization-defective mutants of *Caenorhabditis elegans*. *J. Cell Biol.* 91:26–44.
Ward, S., E. Hogan, and G. A. Nelson. 1983. The initiation of spermiogenesis in the nematode *Caenorhabditis elegans*. *Dev. Biol.* 98:70–79.
Ward, S., T. M. Roberts, S. Strome, F. M. Pavalko, and E. Hogan. 1986. Monoclonal antibodies that recognizes a polypeptide antigenic determinant shared by multiple *Caenorhabditis elegans* sperm-specific proteins. *J. Cell Biol.* 102:1778–1786.
Wolf, N., D. Hirsh, and J. R. McIntosh. 1978. Spermatogenesis in males of the free living nematode *Caenorhabditis elegans*. *J. Ultrastruct. Res.* 63: 155–169.
Wood, W. B. 1988. The nematode *Caenorhabditis elegans*. Cold Spring Harbor Laboratory Press, Cold Spring Harbor, New York. 667 pp.
Yanisch-Perron, C., J. Vieira, and J. Messing. 1985. Improved M13 phage cloning vectors and host strains: nucleotide sequences of the M13Mp18 and pUC19 vectors. *Gene*. 33:103–119.